Predicting the vertical low suspended sediment concentration in vegetated flow using a random displacement model

Wenxin Huai [1], Liu Yang [1], Wei-jie Wang [2], Yakun Guo [3], Tao Wang[1]

[1]State Key Laboratory of Water Resources and Hydropower Engineering Science, Wuhan University, Wuhan, Hubei 430072, China.

[2]State Key Laboratory of Simulation and Regulation of Water Cycle in River Basin, China Institute of Water Resources and Hydropower Research, Beijing 100038, China.

[3]Faculty of Engineering & Informatics, University of Bradford, BD7 1DP, UK.

Highlights:

1. The validity of random displacement model (RDM) to simulate suspended sediment concentration is verified.
2. A concept of integrated sediment diffusion coefficient, which is equal to a coefficient β multiplied by turbulent diffusion coefficient, is introduced to study the dispersion and diffusion in vegetated flow.
3. Results show that β in flow with submerged canopy is larger than that in emergent canopy flow.

Abstract

Based on the Lagrangian approach, this study proposes a random displacement model (RDM) to predict the concentration of suspended sediment in vegetated steady open channel flow. Validation of the method was conducted by comparing the simulated results by using the RDM with available experimental measurements for uniform open-channel flows. The method is further validated with the classical Rouse formula. To simulate the important vertical dispersion caused by vegetation in the sediment-

laden open channel flow, a new integrated sediment diffusion coefficient is introduced in this study, which is equal to a coefficient β multiplying the turbulent diffusion coefficient. As such, the RDM approach for sandy flow with vegetation was established for predicting the suspended sediment concentration in low-sediment-concentration flow with both the emergent and submerged vegetation. The study shows that the value of β for submerged vegetation flow is larger than that for emergent vegetation flow. The simulated result using the RDM is in good agreement with the available experimental data, indicating that the proposed sediment diffusion coefficient model can be accurately used to investigate the sediment concentration in vegetated steady open channel flow.

Keywords: random displacement model, suspended sediment concentration, diffusivity, dispersivity, vegetated sandy flows

1 Introduction

Vegetation and sediments are commonly encountered in rivers and lakes. Aquatic vegetation in rivers has a great impact on the flow characteristics, especially on flow velocity and turbulence (Huai et al., 2009, 2019; Liu et al. 2018). Suspended sediment is of great significance to the ecology and environment in river system. The accurate prediction of sediment transport in vegetated flow, however, is very complex due to complicated interactions between sediments, currents, vegetation (Li et al., 2012), river beds (Joanna, 2013) and riverbank (Samadi et al., 2011; Masoodi et al., 2017, 2019). The sediment diffusion coefficient plays a key role on the transport of suspended sediment. Therefore, it is possible to study the vertical distribution of suspended sediment concentration for estimating the rate of sediment transport for various flow conditions

(Bai & Duan, 2014).

Aquatic vegetation has a blocking effect on flow by increasing hydraulic resistance (Gualtieri et al., 2018), thus reducing the flow velocity and transport capacity of rivers, as well as complicating vertical structure of velocity and turbulence (Stone & Shen, 2002). In submerged vegetated flow, there exist strong velocity shear and turbulence intensities at the top of the canopy due to the vertical discontinuity of the drag force (Ghisalberti & Nepf, 2002; Caroppi et al., 2018). At this zone, the Kelvin-Helmholtz (KH) instability exists and the vortices within the vegetation zone are mixed with the overflow (Raupach et al., 1996), leading to the complex profiles of velocity and diffusivity. Previous studies (Murphy et al., 2007; Nepf & Ghisalberti, 2008; Huai et al., 2009) demonstrate that flow through submerged vegetation can be divided into several layers. In this study, the three-layer model is adopted and will be described in the Section 3.1. Murphy et al. (2007) conducted laboratory experiment to investigate the difference of diffusion coefficient between submerged vegetated flow and non-vegetated flow. They found that the vertical diffusivity in submerged vegetated flow maintained as a constant near the bottom of the river bed and reached the maximum at the top of the vegetation and then approached to zero near the free surface. This conclusion is consistent with the previous studies by Ghisalberti and Nepf (2005). The effect of emergent vegetation on flow characteristics is relatively simpler comparing with the case of submerged vegetated flow. The study of Huai et al (2009) shows that emergent vegetation made the vertical distribution of longitudinal velocity more uniform through the water column. Nepf et al. (1997) investigated the turbulence intensity near the boundary region, i.e., approximately $z < 0.10h$ (where z is the vertical coordinate and h is the flow depth), which region was similar to the condition without vegetation. Their study indicated that the turbulence in this region was mainly derived from the river-bed shear

77 stress rather than from the vegetation wake. In addition, the study on vegetation density
78 and vertical diffusion coefficient shows that the vertical diffusion coefficient increases
79 with the increase of the density for sparse vegetation. When the vegetation density is
80 too high, however, the diffusion coefficient is closely related to the diameter and shape
81 of the vegetation (Nepf, 1999, 2012).

82 There are two main methods to obtain the suspended sediment concentration profile,
83 namely solving the two-phase mixing equation or sediment convection-diffusion equa-
84 tion. Zhong et al. (2015) and Fu et al. (2005) obtained the velocity and sediment con-
85 centration distribution by solving the two-phase mixing equation. However, most stud-
86 ies on sediment concentration distribution are based on solving the following sediment
87 convection-diffusion equation (Lyn, 2006; Cheng et al., 2013; Li et al., 2018):

88 $$K_z \frac{dS}{dz} + \omega S = 0 \qquad (1)$$

89 where K_z is the vertical sediment turbulent diffusion coefficient, S is the suspended
90 sediment concentration, and ω is the settling velocity of sediment particles. Previous
91 studies show that there are two patterns of suspended sediment concentration profile,
92 i.e., Pattern I (Einstein and Chien, 1955; Coleman, 1986) and Pattern II (Bouvard
93 &Petkovic, 1985; Wang and Li, 1990). These two patterns of concentration profile are
94 distinguished from the location of the maximum sediment concentration ($S_{\max}$). Two
95 sediment concertation profile patterns are shown in a schematic diagram Fig. 1, where
96 $a = 0.05h$ is the reference height in non-vegetated sandy flow and S_a represents the
97 referenced sediment concentration at $z = a$. In particular, for the Pattern II concentra-
98 tion distribution, the sediment flux generated by the turbulence, $K_z \frac{dS}{dz}$, cannot reach
99 equilibrium with the sediment flux generated by settling velocity, ωS, in a thin region

near the bottom of channel. This contradicts with the sediment diffusion equation and makes Eq. (1) no solution. Nevertheless, the sediment diffusion equation well illustrates the movement of sediment following turbulent vortices for most conditions. Eq. (1) is based on Fick's first law, therefor, the key point of solving the equation is to appropriately determine the value of the turbulent diffusion coefficient. The effect of suspended sediment on the turbulent diffusion coefficient is often reflected by the turbulent Schmidt number $S_c = \frac{K_m}{K_z}$ or $\beta' = K_z / K_m$ (where K_m is the turbulent diffusion coefficient) in non-vegetated sandy flow. The important coefficient β' is affected by many factors, such as particle size, sediment concentration, velocity and diffusivity of flow, as well as the distance from the bottom of the river-bed (Pal & Ghoshal, 2016).

Rouse (1937) proposed the Rouse formula by assuming $\beta'=1$, which was later proved to be incorrect. The hypothesis $\beta'=1$ is equal to an ideal condition in which the grain movement exactly follows the turbulent current. This assumption can basically be considered to be correct for fine particles, however, it is incorrect for coarse sediments as proved by the study of Graf and Cellino (2002). Absi (2010) reasonably simulated the suspended sediment concentration of fine sediments with a one-dimensional vertical model by assuming the coefficient to be equal to unity and only the effect of particle size was considered in the study. Graf & Cellino (2002) carried out laboratory experiments to show that β' is larger than unity for flow over a flat bed and is smaller than unity for flow over a moveable bed form. The study by Fu et al. (2005) revealed that the traditional study of sediment diffusion equations only considered the gravitational settling and turbulent diffusion, which was only applicable to low-concentration flow with fine grains. Lift force and sediment stress gradient cannot be ignored for high-

concentration flow. In fact, the effect of lift force and sediment stress gradient is significant and should be formulated for predicting sediment dispersion in the region below $0.10h$ (Kallio & Reeks, 1989; Matida et al., 2000). This study focuses on investigating the vertical profile of low suspended sediment concentration within the vegetated uniform flow and thus, the effects of these two items are not considered here.

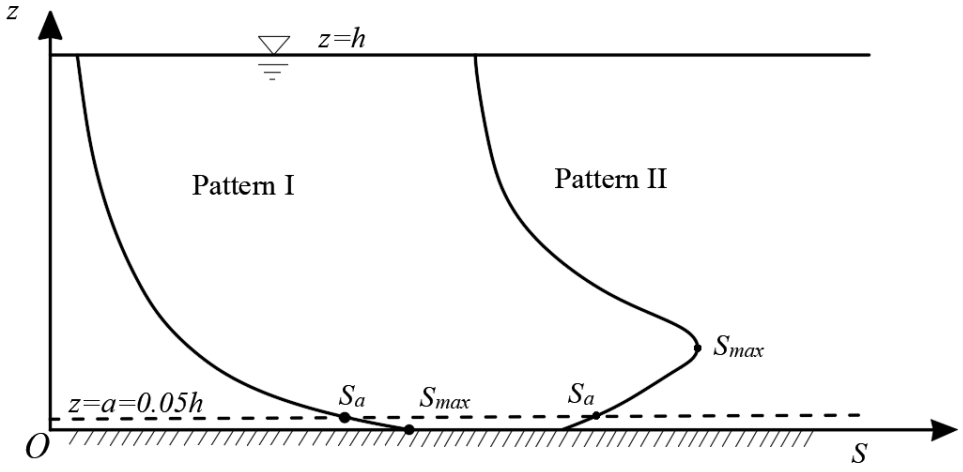

Fig. 1 Schematic diagram of two patterns of suspended sediment concentration profile. Pattern I: Concentration monotonously decrease from the bottom of the river to the free surface (i.e. $\frac{dS}{dz} < 0$); Pattern II: The location of the maximum concentration is not the bottom (i.e. $\frac{dS}{dz} > 0$ in a thin region near the bed).

When the sediment-laden flow moves through the vegetation area, the suspended sediment concentration is significantly reduced (Li et al., 2012), indicating that vegetation has a great effect on the vertical suspended sediment concentration distribution. Therefore, this study is devoted to exploring the influence of vegetation on the suspended sediment concentration in the equilibrium open channel flow by using a Lagrangian mathematical model, i.e., a random displacement model (RDM). To the best

knowledge of the authors, it is the first time to apply the RDM to investigate the suspended sediment transport in vegetated, steady open channel flow. The sediment concentration profile in unsteady flow is much more complex, and there are some numerical models proposed for such situation (Sabbagh-Yazdi, 2013; Zhang et al., 2013; Di Cristo et al., 2016), which differs from this study.

2 Random Displacement Model (RDM)

2.1 Concept

The random displacement model (RDM) is a Lagrangian method. The RDM differs from the Euler method and is based on the study of particles by tracking each discrete particle within the sediment-laden flow (Visser, 1997; Ross & Sharples, 2004). Currently, the RDM method is widely used to investigate the pollutant diffusion in open channels (Salamon & Fernandez-Garcia, 2006; Liang et al, 2014; Liu et al., 2018) and in the porous media (Gray et al., 2016). This is because the RDM can well represent the process of the pollutant diffusion and can be used to accurately calculate the diffusivity.

This study applies the RDM to investigate the sediment diffusion in vegetated flow, providing a new approach for study of suspended sediment concentration. In the simulation of the sediment transport in open channel flow, sediments are represented by numerous discrete particles (represented by n). The distribution of suspended sediment concentration in vegetated flow is then obtained by statistical methods. For simplification, this study considers a two-dimensional (2D) problem, i.e. the vertical z, and longitudinal x with w and u representing the time-averaged vertical and longitudinal flow velocity, respectively. In each constant time step, Δt, these particles move in the domain according to the following rules: The displacements (Δx and Δz) of the par-

ticle is decomposed into two components: the advection term and the probabilistic diffusion term (random displacement). The longitudinal displacement mainly depends on the time-averaged longitudinal velocity u; while the vertical displacement depends on both the particle settling velocity (ω_i) and turbulent velocity (w'). The equations used to simulate the particle position are (Follett et al., 2016):

$$x_{i+1} = x_i + u(z_i) \cdot \Delta t \quad (2)$$

$$z_{i+1} = z_i + (\frac{\mathrm{d}K_z}{dz}(z_i) - \omega_i)\Delta t + R\sqrt{2K_z(z_i)\Delta t} \quad (3)$$

where R is a random number conforming a normal distribution with mean 0 and standard deviation 1, the last term in Eq. (3) represents the transport by turbulent velocity $w' = R\sqrt{\frac{2K_z(z_i)}{\Delta t}}$. The vertical transport includes a pseudo-velocity related to the vertical variation in diffusivity ($\frac{dK_z}{dz}$), which prevents the artificial accumulation of particles owing to low diffusivity (Boughton et al., 1987; Wilson & Yee, 2007). The concentration at a certain position and time t can be obtained by counting the number of particles in the volume after computing the positions of particles based on Eqs. (2) and (3). The physical concept is clarified in the schematic diagram shown in Fig. 2. The expressions of $u(z)$ and $K_z(z)$ will differ depending on different hydraulic conditions, and will be discussed in the following sections.

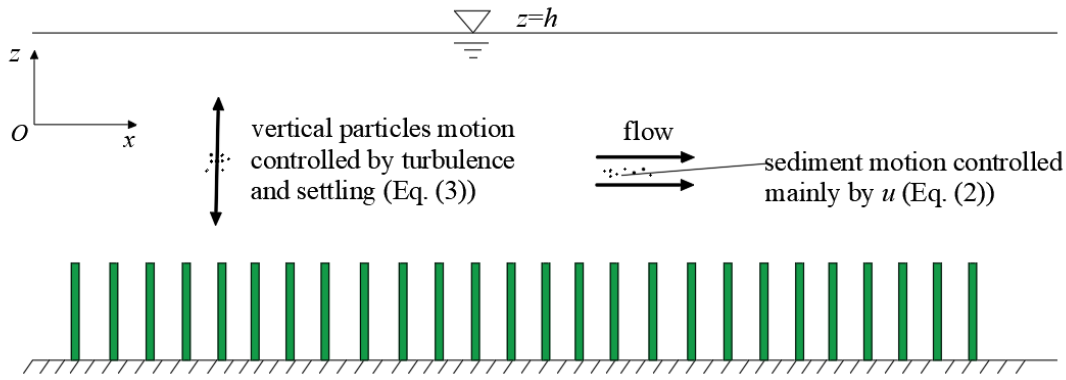

Fig. 2 The schematic diagram of the RDM approach (governed by Eqs. (2) and (3))

According to Israelsson et al. (2006) and Follett et al. (2016), the model time step, Δt is restricted to the region of the vertical particle excursion within each time step that is much smaller than the scale of the vertical gradient in the diffusivity and velocity. This means that when the time step is too large, there will be a large deviation of the particle position calculated at the next time step by using the flow velocity and diffusion coefficient at the previous time step. Both the velocity and diffusivity vary over length scales of approximately $0.05h$. Therefore, the formula for determining time step is:

$$\Delta t < \min\left(\frac{0.05h}{\left|\frac{dK_z}{dz}-\omega\right|_{\max}}, \frac{(0.05h)^2}{(K_z)_{\max}}\right) \tag{4}$$

Assume that no bed load is present and reflecting boundary conditions are applied at the bottom of channel (Eq. (5)) and on the water surface (Eq. (6)):

$$z_i = -z_i, \quad z_i < 0 \tag{5}$$

$$z_i = 2h - z_i, \quad z_i > h \tag{6}$$

2.2 Validation of RDM using classical Rouse formula

To demonstrate the reliability of the RDM method for simulating sediment concentration, the model is firstly validated by comparing with the classic Rouse formula.

The velocity distribution of clear water flow is usually in the form of logarithmic distribution for uniform open-channel flow:

$$u(z) = \frac{u_*}{k} \ln\left(\frac{30.0z}{z_0}\right) \tag{7}$$

where the von Karman's constant $k = 0.40$ in the clear water flow, friction velocity $u_* = \sqrt{gsh}$ (g is the acceleration due to gravity, s is the slope of channel), and z_0 is the roughness height.

Rouse assumed that the sediment diffusion coefficient was equal to the turbulent diffusion coefficient, i.e. $K_z = K_m$ (Rouse, 1937). K_z can be estimated from the sediment diffusion equation:

$$K_z = k u_* z \frac{h - z}{h} \tag{8}$$

The Rouse formula can then be expressed as:

$$\frac{S}{S_a} = \left(\frac{h - z}{z} \cdot \frac{a}{h - a}\right)^{\varphi} \tag{9}$$

where a is the reference height, generally taking as $a = 0.05h$ and S_a is the suspended sediment concentration at the reference height. The suspension index $\varphi = \frac{\omega}{k u_*}$ reflects the relative magnitude of gravity and turbulent diffusion intensity. For large φ, the gravity effect is strong and the suspended sediment will be mostly centralized not far from the bottom, leading to more uneven equilibrium sediment concentration vertically. For small φ, the turbulence intensity is strong, and more sediment can be brought to a position far away from the riverbed, which results in a much more uniform vertical equilibrium suspended sediment concentration profile. In this study, we con-

sider seven cases of $\varphi = \frac{1}{32}, \frac{1}{16}, \frac{1}{8}, \frac{1}{4}, \frac{1}{2}$, 1 and 2. The corresponding settling velocity can be calculated as $\omega = \varphi k u_*$, the number of particles $n = 10^5$, and the time step $\Delta t = 0.05$ s, which meets the requirement of Eq. (4), $h = 0.34$ m, $z_0 = 0.01$ m and $s = 0.02$.

Even in the case of known velocity and turbulent field, significant computing resources are required to track the positions of many particles for each computational time step. Therefore, it is very important to optimize the computational time by reducing the unnecessary computational time. The computational time should satisfy the equilibrium state of the sediment transport. The root-mean-square error (*RMSE*) is used to determine whether the balance of the model is statistically met. When statistical balance is reached, the sediment transport can be considered to reach the equilibrium state.

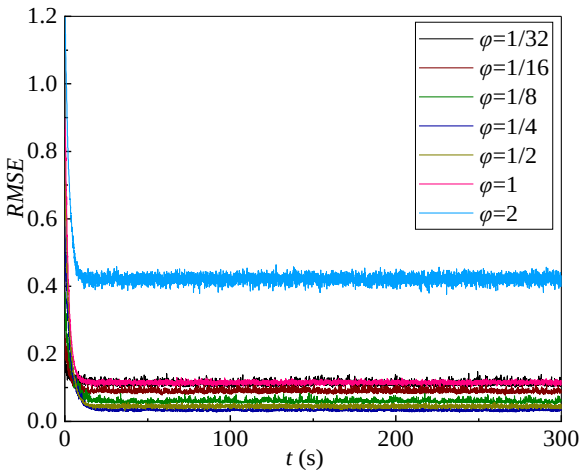

Fig. 3 The variation of *RMSE* with computational time.

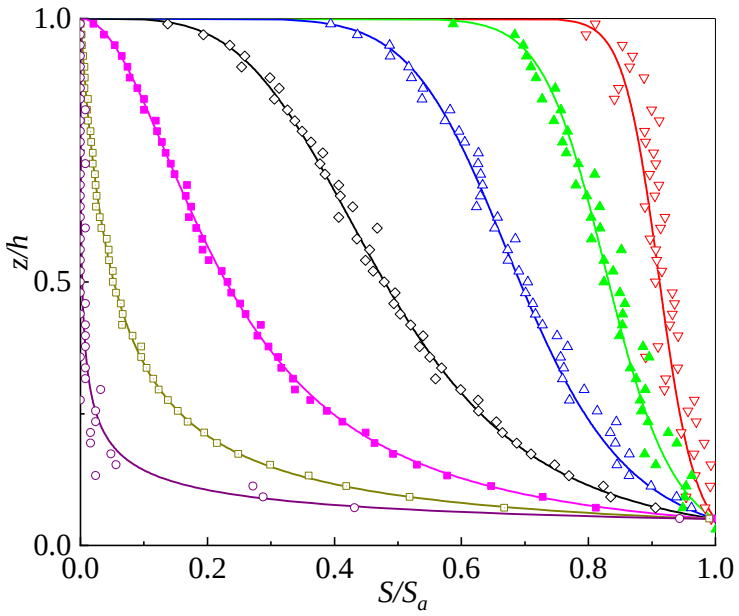

Fig. 4 Comparison of the Rouse formula and the RDM, where solid lines indicate the results of the Rouse formula and symbols indicate the simulation by the RDM. Symbols: ▽: $\varphi=\frac{1}{32}$; ▲: $\varphi=\frac{1}{16}$; △: $\varphi=\frac{1}{8}$; ◇: $\varphi=\frac{1}{4}$; ■: $\varphi=\frac{1}{2}$; □: $\varphi=1$; ○: $\varphi=2$.

The root-mean-square error (*RMSE*) is expressed as

$$RMSE=\sqrt{\frac{\sum_{i=1}^{N}(C_i-R_i)^2}{N-1}} \tag{10}$$

where N is the total number of sampling point, C_i is the sediment concentration calculated by the RDM, and R_i is the concentration calculated by the Rouse formula for the corresponding concentration position. When the *RMSE* value tends to be stable, the sediment transport can be considered to have reached the equilibrium state. Fig. 3 shows the variation of *RMSE* with the computational time. It can be seen from Fig. 3 that when $t>30$ s the simulated sediment transport for all values of φ reaches an

equilibrium state. The time calculated in this paper is 100 s, which meets the requirement for equilibrium state.

Fig. 4 is the comparison between the simulated suspended sediment concentration by using the RDM method with those calculated by using the Rouse formula. Fig. 4 shows that in general, the calculated suspended sediment concentration by using the RDM method agrees well with those using the Rouse formula. Some relatively large discrepancy between two methods can be found for large φ (φ=2). Interaction of particles may account for such deviation.

2.3 Verification of RDM using the data of Einstein and Chien (1955)

The Rouse formula was obtained by assuming that the sediment concentration at the bottom of the river bed is infinite and zero on the water surface, which was not true. The RDM method is thus further verified by comparing with the experimental data of Einstein and Chien (1955), which were two-dimensional, fully developed steady open-channel flows. These data are employed not only to verify the present model, but also to further analyze the sediment dispersion. The experimental parameters are listed in Table 1. As discussed above, the sediment concentration has an influence on the flow velocity and turbulent diffusion coefficient, which will change the von Karman's constant in the sediment laden flow. As such, the von Karman's constant obtained from various experimental conditions (Einstein and Chien 1955, see Table 1) are used in the simulation.

Table 1 Flow and Sediment Characteristics in experiment of Einstein and Chien (1955).

Run number	h (cm)	d (10^{-3}m)	u_* (cm/s)	$S_a(0.10h)$ (%)	ρ_s / ρ_f	k
S11	13.3	0.274	10.61	0.40	2.65	0.380
S12	13.2	0.274	10.09	1.98	2.65	0.278
S13	13.4	0.274	10.50	2.94	2.65	0.247
S14	12.4	0.274	12.12	5.10	2.65	0.255
S15	12.4	0.274	11.98	9.10	2.65	0.219

Note: ρ_s and ρ_f represent the density of sediment and water, respectively; d is the size of sediment particle.

The particle settling velocity is very important in investigating the suspended sediment concentration profile. The calculation formula of particle settling velocity differs for various flow conditions. In this study, the formula proposed by Zhang &Xie (1989), which is applicable to flow ranging from laminar to turbulent, is used to calculate the particle settling velocity:

$$\omega=\sqrt{(13.95\frac{\nu}{d})^2+1.09\frac{\gamma_s-\gamma_f}{\gamma_f}gd}-13.95\frac{\nu}{d} \tag{11}$$

where ν represents the kinematic viscosity of water; γ_s and γ_f represent the bulk density of sediment and water, respectively.

Sediment settling velocity can be affected by particle interaction for higher suspended sediment concentration (Chine and Wan 1999). However, in this study the suspended sediment concentration is low (< 7%), the effect of sediment concentration on the particle settling velocity can thus be ignored (Bagnold 1954).

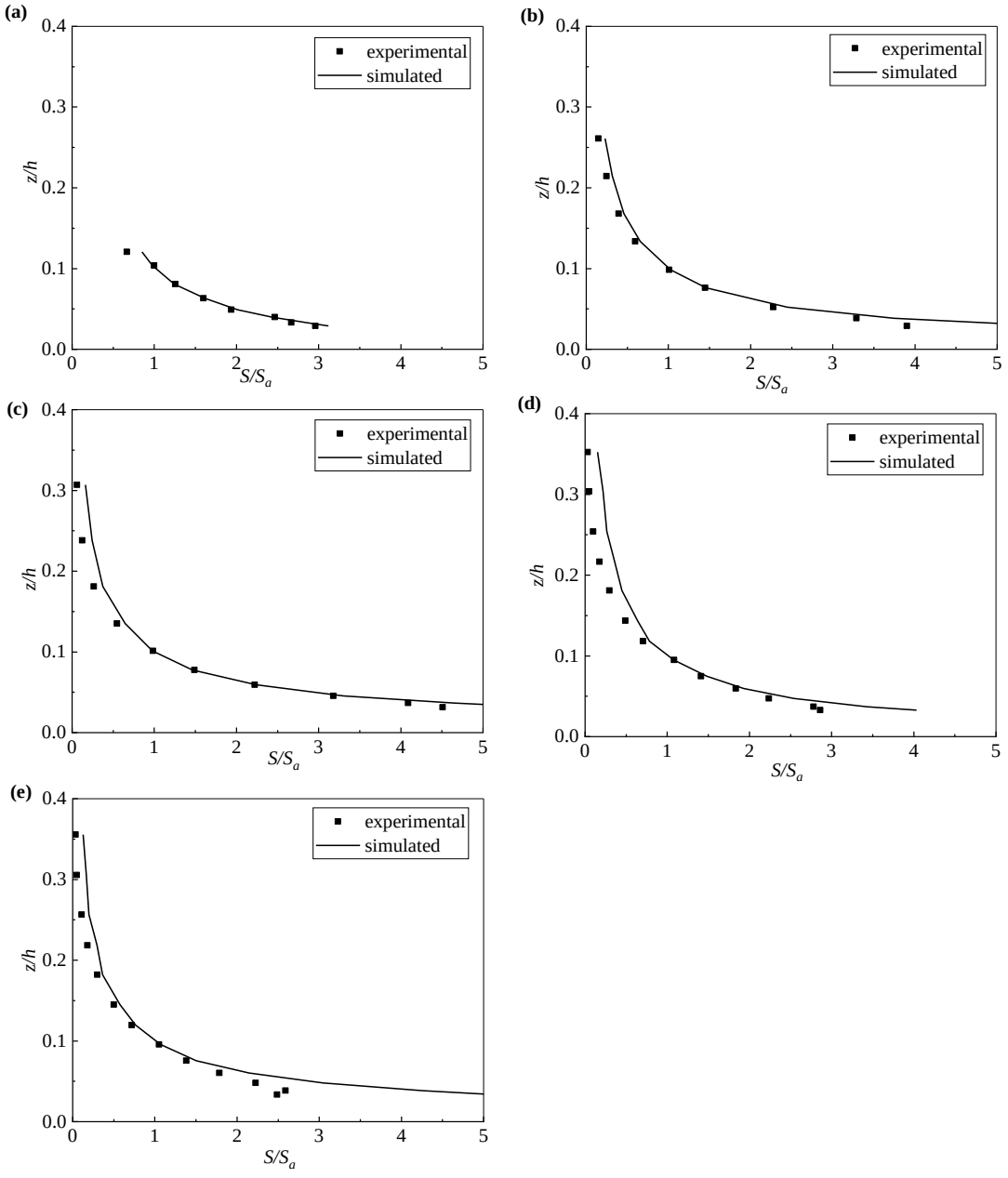

Fig. 5 Comparison of the simulated and measured suspended sediment concentration for uniform open channel flow: (a) profile S11; (b) profile S12; (c) profile S13; (d) profile S14; (e) profile S15.

Fig. 5 shows the comparison of the simulated suspended sediment concentration distribution by the RDM method with the experimental results. It is seen from Fig. 5 that the model can well predict the suspended sediment concentration. While there exists

some slight deviation between the simulated and measured sediment concentration near the bottom of the river bed where the interaction between sediments and river bed is complex. Given the complexity of the problem under investigation, it can be concluded that the RDM method is capable of simulating the suspended sediment transport in open channel flow without vegetation with satisfactory accuracy. This provides a new method for the general solution of the sediment convection-diffusion equation, which is difficult to obtain analytical solution.

3 Suspended sediment concentration in flow with vegetation

This section will examine the application of the RDM method in simulating the sediment-laden flow with vegetation. For open channel flow without aquatic vegetation, the dispersion is much smaller than the diffusion, and Eq. (1) can thus be adopted to describe the suspended sediment concentration. However, for open channel flow with aquatic vegetation, the presence of vegetation greatly enhances the inhomogeneity of vertical profile of flow velocity. In this case, the dispersion is the same order as the diffusion. Therefore, it is essential to include the dispersion term in the governing equation. Applying the double-averaging method in vegetated steady flow (Poggi et al., 2004; Termini, 2019), Eq. (1) can then be modified as:

$$-K_z \frac{dS}{dz} + \langle w'' S'' \rangle = \omega S \tag{12}$$

where w'' represents the vertical time averaged velocity's deviation from the spatial mean velocity $\langle w \rangle$ and S'' is the time averaged suspended sediment concentration's deviation from the spatial mean concentration. Therefore, the second term on the left-hand side of Eq. (12) is a dispersion term with spatial heterogeneity in the time-mean velocity field. Poggi et al. (2004) demonstrated that the dispersion flux is usually smaller than diffusion flux and can be ignored in clear water flow ($S''=0$). Eq. (12),

however, shows that the dispersion flux can be enhanced by the heterogeneous profile of sediment concentration.

The dispersion flux $\langle w"S"\rangle$ can be estimated as:

$$\langle w"S"\rangle = -K_{zp}\frac{dS}{dz} \tag{13}$$

where K_{zp} represents the sediment dispersion coefficient. Defining the integrated sediment turbulent diffusion coefficient K_z' as following:

$$K_z' = K_z + K_{zp} \approx \beta K_m \tag{14}$$

where the coefficient β includes the effect of diffusion and dispersion in vegetated sandy flow. Many factors, such as sediment concentration, particle diameter (Pal & Ghoshal, 2016) and canopy density, influence the coefficient β.

To propose the expression of integrated sediment turbulent diffusion based on the turbulent diffusion coefficient of clear water flow and coefficient β, this study applies the RDM method to simulate suspended sediment concentration of the sandy flow with emergent and submerged vegetation respectively and compares the simulated results with available experimental data.

3.1 Flow with emergent vegetation

Previous study (Huai et al., 2009) shows that emergent vegetation can make the flow field tend to be uniform. The velocity is approximately constant in the outer region and changes slightly in the viscous region near the river bed. The vegetation drag force and gravity are the main effects in the outer region, where other forces are relatively smaller and can be ignored. The velocity is then derived as follows:

$$u_1 = \sqrt{\frac{2gs}{C_D a_v}} \tag{15}$$

where C_D is the drag coefficient ($C_D = \frac{2gs}{a_v u_1^2}$ according to Eq. (15)), a_v is the canopy frontal area per volume. Because the viscous boundary region is always thin, the outer region dominates the velocity of the flow field in emergent vegetated flow. In this study the averaged longitudinal velocity is approximated as u_1.

Similarly, the turbulent diffusion coefficient of flow with emergent vegetation is generally evenly distributed. Nepf (2004) theoretically and experimentally studied the turbulent diffusion coefficient of emergent vegetation, and proposed the diffusion coefficient as follows:

$$K_m = \alpha \sqrt[3]{C_D a_v D} UD \tag{16}$$

where U is the averaged flow velocity in the cross-section, D is the diameter of vegetation stem and α is a proportional factor, which is taken as 0.2 for the vertical turbulent diffusion coefficient and as 0.8 for the lateral turbulent diffusion coefficient in the emergent vegetated flow.

To consider the effect of dispersion on the vertical suspended sediment concentration distribution in vegetated flow, substituting Eq. (16) into Eq. (14) yields:

$$K_z' = \beta K_m = \beta\alpha \sqrt[3]{C_D a_v D} UD \tag{17}$$

Table 2 Experimental parameters, drag coefficient and determined coefficient β in emergent-canopy flow.

Run number	h (m)	D (m)	s (10^{-3})	U (m/s)	u_* (m/s)	R_e (10^4)	a_v (m^{-1})	C_D	β
D12-1	0.12	0.006	13.6	0.3343	0.1265	3.1	2.4	0.9938	2.1
D12-2	0.12	0.006	13.6	0.2918	0.1265	2.7	3.0	1.0435	2.0

D12-3	0.12	0.006	13.6	0.1690	0.1265	1.6	6.0	1.5555	2.1
D15-1	0.15	0.006	13.6	0.3321	0.1414	3.5	2.4	1.0070	2.1
D15-2	0.15	0.006	13.6	0.2932	0.1414	3.1	3.0	1.0336	2.0
D15-3	0.15	0.006	13.6	0.1700	0.1414	1.8	6.0	1.5373	2.0
D18-1	0.18	0.006	13.6	0.3436	0.1549	4.0	2.4	0.9408	2.1
D18-2	0.18	0.006	13.6	0.2947	0.1549	3.5	3.0	1.0231	2.2
D18-3	0.18	0.006	13.6	0.1692	0.1549	2.0	6.0	1.5518	2.0

We attempt to derive the vertical integrated sediment turbulent diffusion coefficient of sediment-laden flow with emergent vegetation by fitting β with the experimental data. To ensure the accuracy of the coefficient, interference of other factors should be excluded. It is well known that the value of C_D changes slightly with the vegetation density. Therefore, to eliminate the influence of the drag coefficient, we calculate C_D by assuming that u_1 in Eq. (15) is equal to the averaged velocity in the cross-section *U*. The results of the experimental parameters of the emergent canopy flow (Lu, 2008) and the calculated drag coefficient are listed in Table 2 in which the size of sediment d is 0.217 mm and reference height $a = 0.50h$.

To choose the best fitting results, the mean relative error (*MRE*) is used to evaluate the fitting effect of the simulation and measurement:

$$MRE = \frac{\sum \frac{|C_i - O_i|}{O_i}}{N} \times 100\% \tag{18}$$

where O_i is the observed sediment concentration in the experiments and definition for other parameters can be found below Eq. (10). Eq. (18) shows that large *MRE* implies

that the error between simulation and observation is large. Therefore, β will be selected as the best-fitting coefficient for the relationship of K_z' and K_m when *MRE* reaches the smallest value. The simulated results for *MRE* with β are shown in Fig. 6. It can be seen that the value of *MRE* first decreases and then increases with the increase of β. For each case, β is then chosen at the lowest point of the curve.

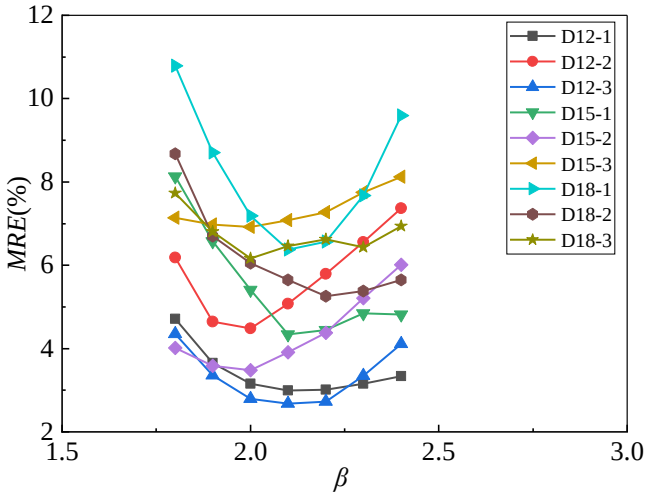

Fig. 6 Variation of the mean relative error (*MRE*) with parameter β in emergent-canopy flow.

The coefficient β fitted from experiments is shown in Table 2 and plotted in Fig. 7 against experimental runs. Table 2 and Fig. 7 demonstrate that β doesn't change significantly under the conditions of the experiment tested, with an averaged value of 2.1 for all experiments. This could be the consequence of spatial inhomogeneity enhanced by the presence of vegetation.

For the fitted coefficient β, the comparison between the simulated by the RDM method and measured (Lu, 2008) suspended sediment concentration is shown in Fig. 8. Fig. 8 shows that the prediction of the suspended sediment concentration by the proposed model, in general, agrees well with the measurements. Some discrepancy

399 in the near bed between the simulations and measurements is seen to take place. This
400 discrepancy may be ascribed to the fact that the sediment tested in the laboratory
401 experiments was not completely uniform, meaning that the suspended sediment near
402 the bottom was coarser than the median size of sediments above the bed. Eventually,
403 this will lead to the underestimation of suspended sediment concentration in the near
404 bed region by the model where the median size of sediment was used.
405

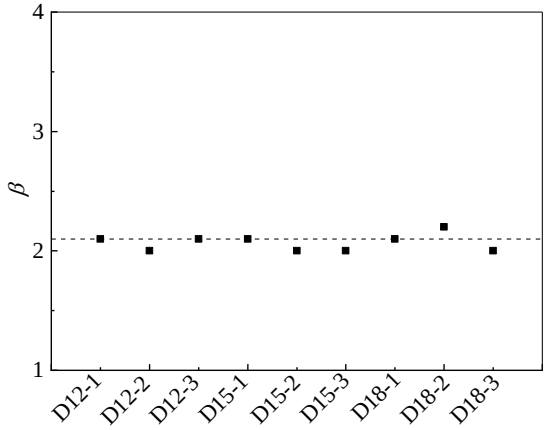

406

407 **Fig. 7** The change of β factor for nine experimental conditions in emergent-canopy
408 flow.
409

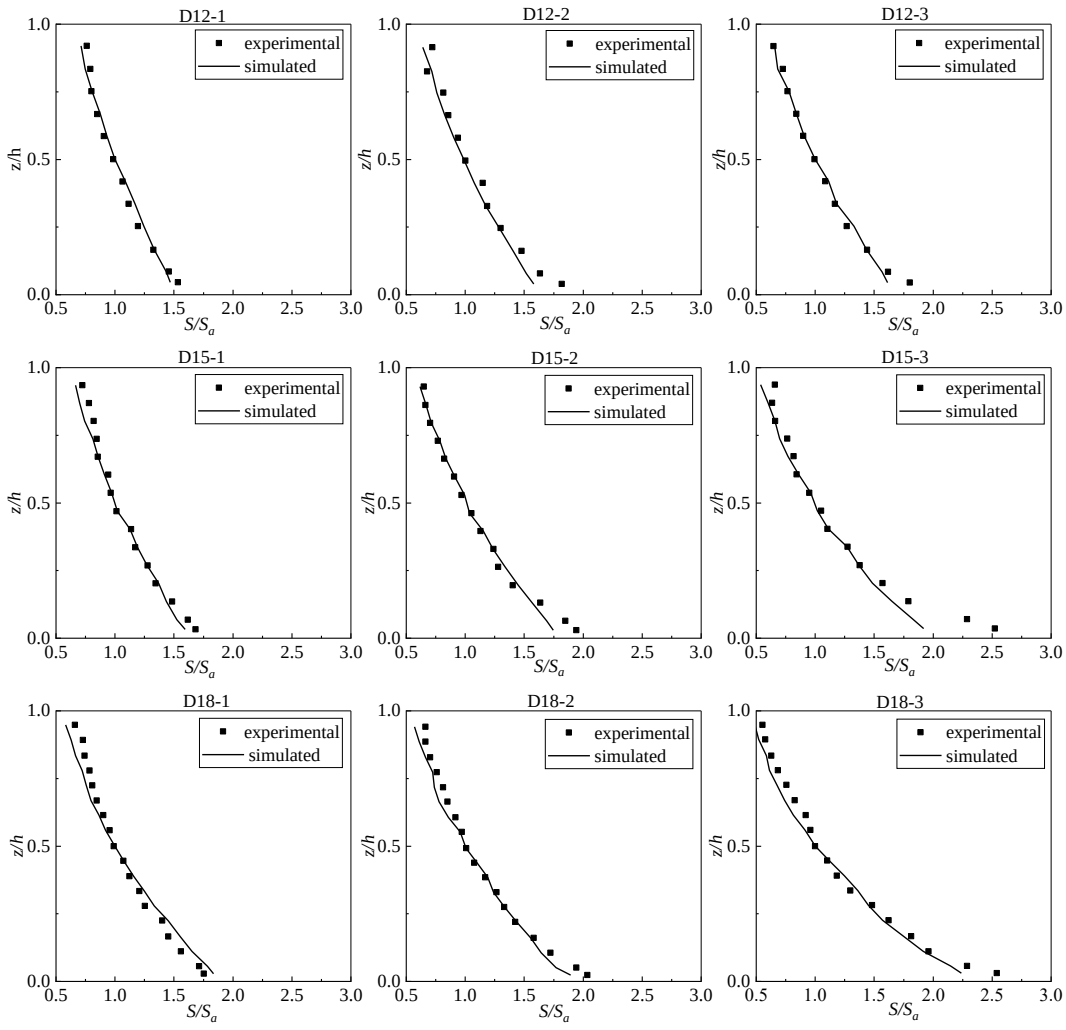

Fig. 8 Comparison of the measured (Lu, 2008) and simulated normalized suspended sediment concentration in emergent vegetated flow.

3.2 Flow with submerged vegetation

Submerged vegetation is commonly found in rivers, which greatly changes the suspended sediment transport and its vertical distribution. Therefore, it is of great importance to study the distribution of suspended sediment concentration in submerged vegetated flow. The velocity and turbulent diffusivity of flow with submerged vegetation is complex. According to Nepf and Ghisalberti (2008), flow is divided into three

layers vertically. For a dense canopy (i.e. $a_v h_v > 0.10$ where h_v represents the vegetation height), the flow velocity and turbulent diffusion coefficient for each layer are expressed as follows (Nepf, 2012):

In the overflow zone ($z \geq h_v$), the velocity profile is approximately logarithmic:

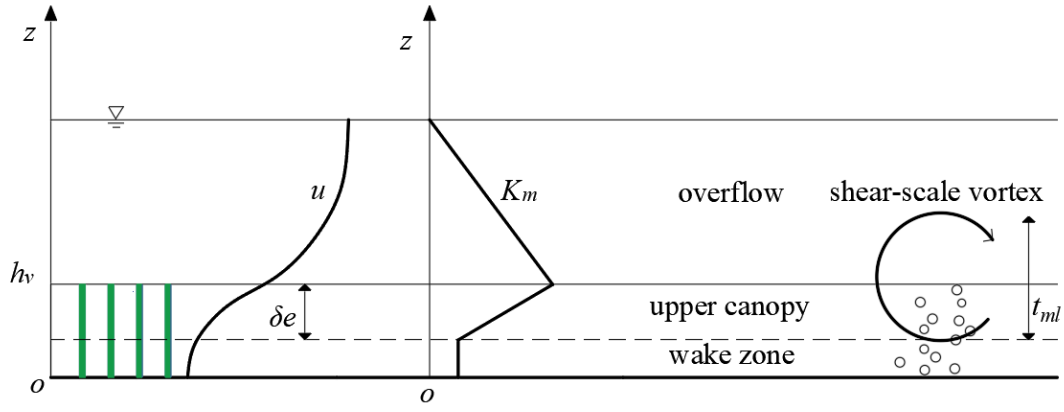

Fig. 9 The vertical distribution of velocity and turbulent diffusivity in submerged-canopy flow.

$$u(z) = \frac{u_*}{k} \ln\left(\frac{z - z_m}{z_0}\right) \tag{19}$$

where z_m and z_0 are the displacement and roughness height, respectively. The displacement height is the centroid of momentum penetration into the canopy (Thom, 1971):

$$z_m = h_v - \frac{\delta_e}{2} \tag{20}$$

where the penetration length scale δ_e is the distance to which turbulent vortex penetrates the canopy. In the range $C_D a_v h_v = 0.10$ to 0.23, the penetration length can be calculated as:

$$\delta_e = \frac{0.23 \pm 0.06}{C_D a_v} \tag{21}$$

The roughness height depends on the effective height, rather than the canopy height, so that $z_0 \propto \delta_e \propto a_v^{-1}$. For example, for $a_v h_v > 0.10$ (i.e. dense canopy), the roughness height can be evaluated as:

$$z_0 = \frac{0.04 \pm 0.02}{C_D a_v} \tag{22}$$

In the upper canopy zone ($h_v - \delta_e < z < h_v$), velocity is driven by both potential gradients and turbulent stress. The time-averaged velocity is:

$$u(z) = u_1 + (u_h - u_1)\exp(-K_u(h_v - z)) \tag{23}$$

where the coefficient $K_u = (8.7 \pm 1.4) C_D a_v$ according to Nepf (2012), and u_1 is the velocity in the wake zone, u_h is the velocity at $z = h$ and can be obtained from Eq. (19).

The third zone is the wake zone ($z \le h_v - \delta_e$), in which the velocity u_1 is almost a constant that can be described by Eq. (15).

The vertical turbulent diffusion coefficient K_m is based on previous research (Murphy et al., 2007; Nepf & Ghisalberti, 2008). Experimental studies show that for dense vegetation the vertical vortices development is limited by the vegetation in the wake region. The vertical transport is mainly controlled by the turbulence generated by the vegetation wake. The turbulent diffusion coefficient in the wake zone is:

$$K_m = 0.17 u_1 D \tag{24}$$

The turbulence intensity reaches a maximum at the top of the canopy and then gradually decreases towards the water surface. The turbulent diffusion coefficient at $z = h_v$ is (Ghisalberti & Nepf, 2005):

$$K_m\Big|_{z=h_v} = 0.032\Delta u \cdot t_{ml} \tag{25}$$

where Δu is the velocity difference at the water surface and the wake region of the vegetated flow (i.e. $\Delta u = u_h - u_1$), and t_{ml} is the thickness of the mixing layer (Ghisalberti & Nepf, 2002), which is in general equal to vegetation height (i.e. $t_{ml} \sim h_v$). For simplification, we use an approximate method to express K_m: (1) calculating the maximum value of K_m using Eq. (25) and the value in the wake region using Eq. (24); (2) approximating the diffusion coefficient equal to zero at the water surface and a linear transition is assumed in the upper canopy and overflow, respectively. The vertical distribution of K_m and $u(z)$ is then approximated as shown in Fig. 9.

To validate the model, the experiments of Lu (2008) and Wang et al. (2016) are used, whose experimental parameters are listed in Table 3. These experiments were conducted with low sediment-concentration. The size of sediment d and reference height are 0.217 mm and 0.50h, respectively.

Table 3 Experimental parameters in submerged-canopy flow.

Sources	Run number	h (cm)	h_v (cm)	D (m)	S (10^{-3})	u_* (cm/s)	Re (10^4)	a_v (m^{-1})	β
Lu	C12	12	6	0.006	4.65	4.76	3.0	3	2.8
	C15	15	6	0.006	3.50	4.77	3.5	3	2.9
	C18	18	6	0.006	2.69	5.20	4.1	3	2.8
	C24	24	6	0.006	1.35	4.45	4.1	3	2.9
	C30	30	6	0.006	0.83	3.71	4.5	3	2.7
Wang	SSW	35	25.1	0.002	0.51	2.23	0.0495	0.9	2.8

Note: Q and R_e represent the flow rate and Reynolds number, respectively. The Re in Wang's experiment is stem Reynolds number, $R_e = DU/\nu$.

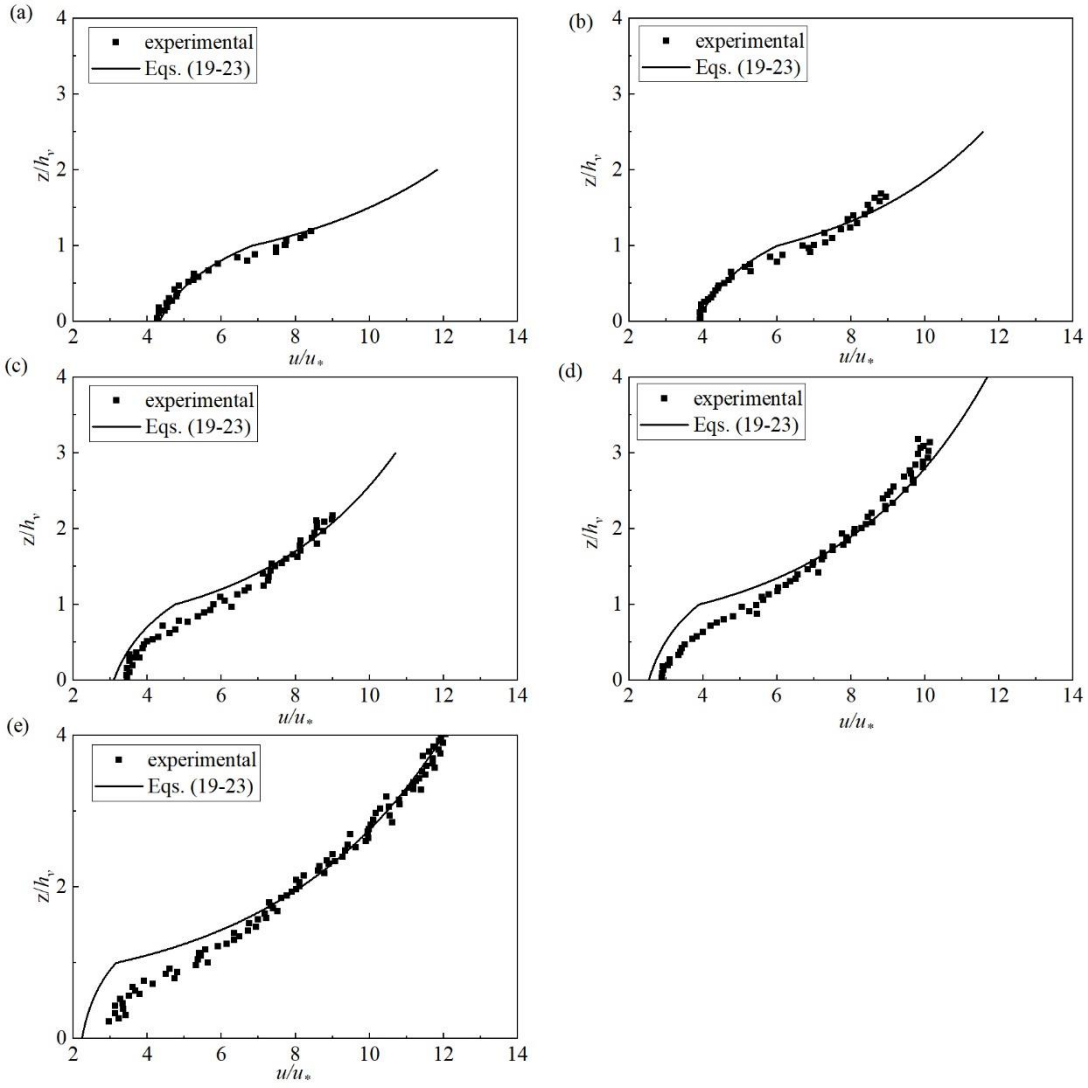

Fig. 10 Comparison of the simulated (by Eqs. (19-23) and measured normalized velocity profiles in submerged-canopy flow: (a) profile C12; (b) profile C15; (c) profile C18; (d) profile C24; (e) profile C30.

The integrated sediment turbulent diffusion coefficient K_z' with submerged canopy sandy flow can be obtained from Eq. (14). Fig. 10 shows the comparison of the calculated and measured velocity profile for various flow conditions. It is seen that the

simulated results agree well with the measurements, particularly in the overflow region which is less affected by canopies. Some deviation between simulation and measurement takes place in the wake and upper canopy regions, where the flow structure is significantly affected by wake structures induced by vegetation. The presence of sediment has the effect to smoothen the vertical velocity distribution, leading to the underestimation of Eqs. (19-23), which are obtained from clear water flow, at the region near the bed and overestimation near the water surface.

The simulated results of *MRE* with β are shown in Fig. 11. The rule of *MRE* and β here is the same as that in the flow with emergent canopy. Values of β can be chosen from Fig. 11 at the lowest points of each curve and are listed in Table 3 and plotted in Fig. 12. Results show that the coefficient β is almost constant with an averaged value of 2.8 for submerged vegetated sandy flow.

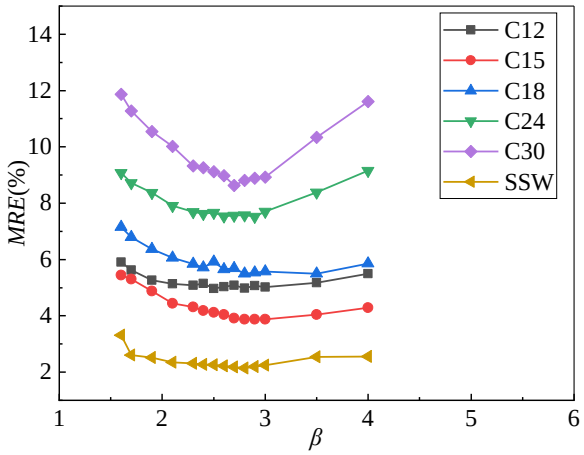

Fig. 11 Variation of mean relative error (*MRE*) with parameter β in submerged-canopy flow.

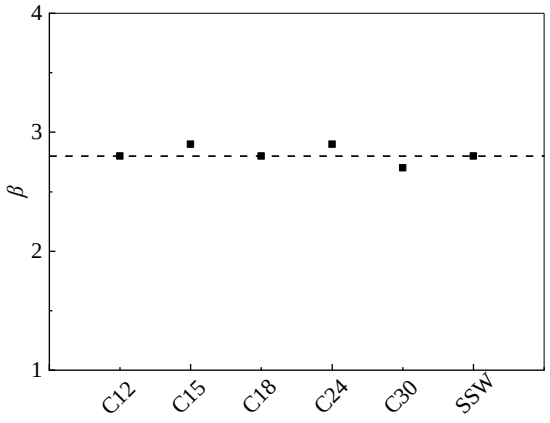

Fig. 12 The change of factor β for six experimental conditions in submerged-canopy flow.

Fig. 13 shows the comparison of the simulated and measured normalized suspended sediment concentration for runs C12-C30 and SSW. In general, simulated suspended sediment concentration in submerged vegetation flow is in good agreement with the experimental data in almost all flow regions. Some deviation between the simulation and measurement exists near the bottom of the river bed, where the size of sediments is larger than median diameter used in model. This leads to the underestimation of suspended sediment concentration in the near bed region by using the model. Moreover, it is also difficult to carry out accurate measurement of suspended sediment concentration near the river bed. In general, these results demonstrate that the sediment diffusion model used in this paper can accurately simulate the concentration of suspended sediment in flow with submerged vegetation.

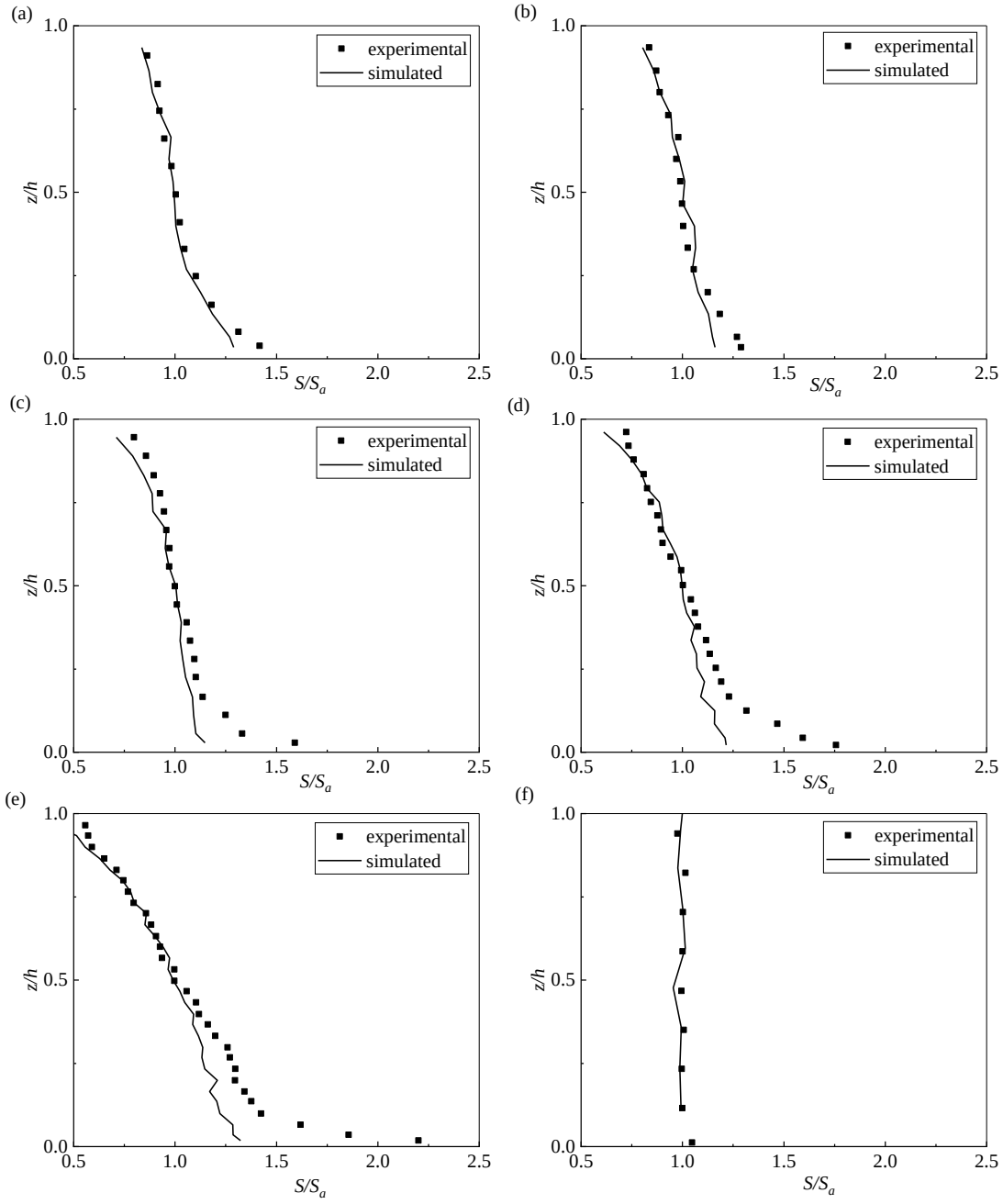

517

518 **Fig. 13** Comparison of measured and simulated profiles of the normalized suspended
519 sediment concentration in submerged-vegetation flow for different conditions: (a) pro-
520 file C12, (b) profile C15, (c) profile C18, (d) profile C24, (e) profile C30, and (f) pro-
521 file SSW.

522

523 **4 Discussions**

524 In this paper, the RDM approach is firstly applied to predict the vertical distribution

of suspended sediment concentration, and the settling velocity of sediment is reasonably considered to distinguish the sediment and the pollutants, which generally ignores gravity. The RDM is validated and verified by comparing the simulated results with the experimental data without and with canopy flow as well as the classical Rouse formula. When applying the model to steady vegetated open channel flow with low sediment concentration, although microscopic movement such as collisions between sediment particles or particles and vegetation are not considered, results show that the RDM method can accurately simulate the flow and suspended sediment concentration profile. From this perspective, the RDM is proven to be one of the effective approaches to study the complex problem of suspended sediment concentration profile.

Owing to the presence of vegetation, the dispersion effect of sandy flow is enhanced, and the mechanism of interaction between sediments, current, vegetation, and river bed becomes much more complicated. The distribution of suspended sediment concentration mainly depends on the interaction between sediment and turbulence. In this study, the RDM is applied to establish the turbulent diffusion model of the sediment-laden flow by fitting coefficient β, which can well simulate the concentration distribution of suspended sediment. It is reasonable to ignore the dispersion coefficient and assume $\boldsymbol{\beta=1}$ for low sediment concentration flow without vegetation (Dohmen-Janssen et al., 2001). When aquatic vegetation exists, the dispersion, which varies greatly for different conditions, has the same order of magnitude as the turbulent diffusion and can be described by Eq. (14). The value of β in Eq. (14) can be obtained by the RDM for flow with both submerged and emergent vegetation. As such, the integrated sediment turbulent diffusion coefficient model K_z' of the flow with vegetation can be constructed, which facilitates solving the interaction between vegetation and sandy flow.

The mechanism that affects the diffusion coefficient of sediment-laden flow is very

550 complicated. van Rijn (1984) proposed parameters that characterized the relationship
551 between sediment diffusion coefficient and turbulent diffusion coefficient in open chan-
552 nel flow without vegetation:

553 $$K_z = \beta_p \phi K_m \tag{26}$$

554 where parameter ϕ describes the effect of the suspended sediment concentration on
555 diffusion, parameter β_p characterizes the influence of sediment particle settling ve-
556 locity on the sediment diffusion coefficient. Results of van Rijn (1984) showed that ϕ
557 was approximated to be unity in low-concentration sediment-laden flow and β_p could
558 be expressed as:

559 $$\beta_p = 1 + 2\left[\frac{\omega}{u_*}\right]^2 \tag{27}$$

560 Equation (27) shows that the value of β_p is always larger than unity and increases
561 with the increase of the particle settling velocity under the same hydraulic conditions.
562 However, the dispersion is not taken into consideration in van Rijn's study. Combining
563 with the above analysis, the coefficient β proposed in this study is more accurate as it
564 considers the influence of dispersion under the action of vegetation and sediments. The
565 results show that the dispersion effect of submerged vegetated flow $\beta = 2.8$ is larger
566 than that of emergent vegetated flow $\beta = 2.1$, which is consistent with the fact that
567 the vertical distribution of the velocity and diffusion coefficients in submerged vege-
568 tated flow is much more uneven than those of in emergent vegetated flow. Furthermore,
569 the modeled results imply that the value of β has no direct relation with the density of
570 vegetation in low sediment concentration flow with an emergent canopy, and is not
571 related to the density and submergence of vegetation in submerged-canopy flow. How-
572 ever, more experiments are needed to explore the law of sediment turbulent diffusivity

in high sediment concentration flow with canopy in which sediment particle interaction should be considered.

5 Conclusions

This study is of great help in further studies of the interaction between sediments and flow with vegetation. The following conclusions can be drawn from this study.

(1) Applying the RDM to investigate the suspended sediment concentration profile in non-vegetated and vegetated open channel flow has avoided the difficulty of solving the sediment diffusion equation. The simulated results are in good agreement with available experimental data. Since the solution of the sediment convection-diffusion equation is complicated when the pattern of velocity and diffusivity are complex, the use of the RDM may provide a new approach to solve this problem.

(2) The presence of vegetation enhances the inhomogeneity of flow field, which means that the dispersity cannot be ignored. This phenomenon is more obvious in sandy vegetated flow. This paper proposes an integrated sediment diffusion coefficient $K_z' = \beta K_m$ to express the comprehensive effect of dispersion and diffusion in the low sediment concentration vegetated flow. From the simulation, β is determined as 2.1 for emergent-canopy sandy flow and 2.8 for submerged-canopy sandy flow.

(3) The solution of the parameter β significantly affects the study of the sediment turbulent diffusion coefficient. To further examine the relationship between the sediment diffusion coefficient and turbulent diffusion coefficient, more detailed experiments are required.

Acknowledgements

The research reported here is financially supported by the Natural Science Foundation of China (Nos. 51439007, 11672213, and 11872285) and the Open Funding of State Key Laboratory of Water Resources and Hydropower Engineering Science (WRHES), Wuhan University (Project No: 2018HLG01). Comments and suggestions made by the Editor, the Associate Editor and three Reviewers have greatly improved the quality of the paper.

Notation

The following symbols are used in this article:

a_v	canopy frontal area per volume
a	reference height
C_D	drag coefficient
C_i	suspended sediment concentration computed by RDM method
d	size of sediment particle
D	diameter of vegetation stem
g	acceleration of gravity
h	flow depth
h_v	vegetation height
k	von Karman's constant
K_m	turbulent diffusion coefficient in clear water flow
K_u	empirical coefficient
K_z	sediment turbulent diffusion coefficient
K_z'	integrated sediment turbulent diffusion coefficient
K_{zp}	sediment dispersion coefficient
MRE	mean relative error
n	the number of discrete particles
N	number of sampling point of the proposed model
O_i	observed suspended sediment concentration in experiments

R	a normally distributed random number with mean 0 and standard deviation 1
R_e	Reynolds number
R_i	suspended sediment concentration computed by Rouse formula
$RMSE$	the root-mean-square error
S	suspended sediment concentration
s	slope of channel
S''	time averaged concentration's deviation from the spatial mean concentration
S_a	sediment concentration at reference height
S_c	turbulent Schmidt number
S_{max}	maximum suspended sediment concentration
t	time
t_{ml}	thickness of the mixing layer
U	average velocity in the cross-section
u_*	friction velocity
u, w	flow velocity of direction x and z, respectively
u_1	velocity in the outer region of emergent vegetated flow or velocity in the wake region of submerged vegetated flow
u_h	velocity in the water surface
w'	vertical turbulent velocity
w''	the vertical time averaged velocity's deviation from the spatial mean velocity
x, z	longitudinal and vertical coordinates, respectively
z_0	roughness height
z_m	displacement height
α	proportional factor
β	coefficient includes the effect of diffusion and dispersion in vegetated sandy flow
β_p	coefficient characterizes the influence of sediment particle settling velocity on the sediment diffusion coefficient
β'	coefficient expresses the effect of suspended sediment on the turbulent diffusion coefficient in non-vegetated sandy flow
γ_f	bulk density of water
γ_s	bulk density of sediment

δ_e	penetration length
Δt	time step
Δu	velocity difference between water surface and the wake region
Δx	displacement in the x-direction
Δz	displacement in the z-direction
v	kinematic viscosity of fluid
φ	suspension index
ϕ	parameter
ω	settling velocity of sediment particles
$\langle w \rangle$	vertical spatial mean velocity

606

607 **References**

608 Absi, R., 2010. Concentration profiles for fine and coarse sediments suspended by
609 waves over ripples: An analytical study with the 1-DV gradient diffusion model.
610 Adv. Water Resour. 33 (4), 411 - 418.
611 https://doi.org/10.1016/j.advwaters.2010.01.006.

612 Bagnold, R.A., 1954. Experiments on a gravity-free dispersion of large solid spheres in
613 a Newtonian fluid under shear. Proc. R. Soc. Lond. Series A. 225, 49-63.
614 https://doi.org/10.1098/rspa.1954.0186.

615 Bai, Y., Duan, J. G., 2014. Simulating unsteady flow and sediment transport in vege-
616 tated channel network. J. Hydrol. 515, 90-102. https://doi.org/10.1016/j.jhy-
617 drol.2014.04.030 .

618 Boughton, B. A., Delaurentis, J. M., & Dunn, W. E., 1987. A stochastic model of particle
619 dispersion in the atmosphere. Bound.-Layer Meteor. 40 (1-2), 147-163.
620 https://doi.org/10.1007/BF00140073.

621 Bouvard, M., & Petkovic, S., 1985. Vertical dispersion of spherical, heavy particles in

622 turbulent open channel flow. J. Hydraul. Res. 24 (3), 221-227.
623 https://doi.org/10.1080/00221688509499373.
624 Caroppi, G., Gualtieri, P., Fontana, N., Giugni, M., 2018. Vegetated channel flows: tur-
625 bulence anisotropy at flow–rigid canopy interface. Geosci. 8(7), 259.
626 https://doi.org/10.3390/geosciences8070259.
627 Cheng, C., Song, Z. Y., Wang, Y. G., & Zhang, J. S., 2013. Parameterized expressions
628 for an improved Rouse equation. Int. J. Sediment Res. 28 (4), 523-534.
629 https://doi.org/10.1016/S1001-6279(14)60010-X.
630 Chien, N., Wan, Z.H., 1999. Mechanics of sediment transport. ASCE Press. N. Y.
631 https://doi.org/10.1061/9780784404003.
632 Coleman N. L., (1986) Effects of suspended sediment on the open channel velocity
633 distribution. Water Resour. Res. 22(10), 1377-1384.
634 https://doi.org/10.1029/WR022i010p01377.
635 Di Cristo, C., Greco, M., Iervolino, M., Leopardi, A., & Vacca, A., 2015. Two-dimen-
636 sional two-phase depth-integrated model for transients over mobile bed. J. Hydraul.
637 Eng. ISSN: 0733-9429, 142(2), P. 04015043-1, 20.
638 https://doi.org/10.1061/(ASCE)HY.1943-7900.0001024.
639 Dohmen-Janssen, C. M., Hassan, W. N., & Ribberink, J. S., 2001. Mobile-bed effects
640 in oscillatory sheet flow. J. Geophys. Res.-Oceans. 106 (C11), 27103-27115.
641 https://doi.org/10.1029/2000JC000513.
642 Einstein, H.A., Chien, N., 1955. Effects of sediment concentration near the bed on the
643 velocity and sediment distribution. M.R.D. Sediment Series, Rep. No. 8, Univ. Of
644 California, Berkeley, Berkeley, Calif., and U.S. Army Corps of Engineering.
645 Follett, E., Chamecki, M., Nepf, H., 2016. Evaluation of a random displacement model
646 for predicting particle escape from canopies using a simple eddy diffusivity model.

Agric. For. Meteorol. 224, 40-48. https://doi.org/10.1016/j.agrformet.2016.04.004.

Fu, X., Wang, G., Shao, X., 2005. Vertical dispersion of fine and coarse sediments in turbulent open-channel flows. J. Hydraul. Eng. 131 (10), 877-888. https://doi.org/10.1061/(ASCE)0733-9429(2005)131:10(877).

Ghisalberti, M., Nepf, H., 2005. Mass transport in vegetated shear flows. Environ. Fluid Mech. 5 (6), 527-551. https://doi.org/10.1007/s10652-005-0419-1.

Ghisalberti, M., Nepf, H. M., 2002. Mixing layers and coherent structures in vegetated aquatic flows. J. Geophys. Res.-Oceans. 107 (C2), 3-1-3-11. https://doi.org/10.1029/2001JC000871.

Graf, W. H., Cellino, M., 2002. Suspension flows in open channels; experimental study. J. Hydraul. Res., 40 (4), 435-447. https://doi.org/10.1080/00221680209499886.

Gray, F., Cen, J., Shah, S., Crawshaw, J., Boek, E., 2016. Simulating dispersion in porous media and the influence of segmentation on stagnancy in carbonates. Adv. Water Resour. 97, 1-10. https://doi.org/10.1016/j.advwtres.2016.08.009.

Gualtieri, P., Felice, S. D., Pasquino, V., Doria, G. P., 2018. Use of conventional flow resistance equations and a model for the Nikuradse roughness in vegetated flows at high submergence. J. Hydrol. Hydromech. 66(1), 107-120. https://doi.org/10.1515/johh-2017-0028.

Huai, W. X., Chen, Z. B., Han, J., Zeng. Y. H., 2009. Mathematical model for the flow with submerged and emerged rigid vegetation. J. Hydrodyn. 21 (5), 722-729. https://doi.org/10.1016/S1001-6058(08)60205-X.

Huai, W. X., Zeng, Y. H., Xu, Z. G., & Yang, Z. H., 2009. Three-layer model for vertical velocity distribution in open channel flow with submerged rigid vegetation.

670 Adv. Water Resour. 32 (4), 487-492.
671 https://doi.org/10.1016/j.advwtres.2008.11.014.
672 Israelsson, P. H., Kim, Y. D., Adams, E. E., 2006. A comparison of three lagrangian
673 approaches for extending near field mixing calculations. Environ. Modell. Softw.
674 21 (12), 1631 - 1649. https://doi.org/10.1016/j.envsoft.2005.07.008.
675 Joanna Crowe Curran, W. Cully Hession., 2013. Vegetative impacts on hydraulics and
676 sediment processes across the fluvial system. J. Hydrol. 505, 364-376.
677 https://doi.org/10.1016/j.jhydrol.2013.10.013.
678 Kallio, G., Reeks, M., 1989. A numerical simulation of particle deposition in turbulent
679 boundary layers. Int. J. Multiph. Flow. 15 (3), 433 - 446.
680 https://doi.org/10.1016/0301-9322(89)90012-8.
681 Li, D., Yang, Z. H., Sun, Z., Huai, W. X., Liu, J., 2018. Theoretical model of suspended
682 sediment concentration in a flow with submerged vegetation. Water. 10 (11), 1656.
683 https://doi.org/10.3390/w10111656.
684 Li, J. N., Yang, J. R., Luo, J., 2012. Study on the plants growth effect of the sediment-
685 laden flow turbulence characteristics. Adv. Environ. Sci. Eng. 518-523, 4771-4777.
686 https://doi.org/10.4028/www.scientic.net/AMR.518-523.4771.
687 Liang. D. F, Wu. X. F., 2014. A random walk simulation of scalar mixing in flows
688 through submerged vegetations. J. Hydrodyn. 26(3), 343-350.
689 https://doi.org/10.1016/S1001-6058(14)60039-1.
690 Liu, X.N., Zhou, Q., Huang, S., Guo, Y.K. and Liu, C. 2018. Estimation of flow direc-
691 tion in meandering compound channels. J. Hydrol. 556, 143-153.

https://doi.org/10.1016/j.jhydrol.2017.10.071.

Liu, X. Y., Huai, W. H., Wang, Y., Yang, Z. H., Zhang, J., 2018. Evaluation of a random displacement model for predicting longitudinal dispersion in flow through suspended canopies. Ecol. Eng. 116, 133 - 142. https://doi.org/10.1016/j.ecoleng.2018.03.004.

Lu, S. Q., 2008. Experimental study on distribution law of suspended sediment in water flow of rigid plants (in Chinese), (PhD. dissertation). Hohai University, Nanjing, Jiangsu, China.

Lyn, D. A., 2006. A similarity approach to turbulent sediment-laden flows in open channels. J. Fluid Mech. 193 (193), 1-26. https://doi.org/10.1017/S0022112088002034.

Masoodi, A., Majdzadeh Tabatabai, M.R., Noorzad, A., and Samadi, A., 2017. Effects of soil physic-chemical properties on stream bank erosion induced by seepage in northeastern Iran. Hydrol. Sci. J. 62 (16), 2597-2613. https://doi.org/10.1080/02626667.2017.1403030.

Masoodi, A., Majdzadeh Tabatabai, M.R., Noorzad, A., and Samadi, A., 2019. The Evaluation of Riverbank Stability under the Influence of Soil Dispersion Phenomenon- A Case Study. J. Hydrol. Eng. 24 (3), 05019001-1 to 05019001-10. https://doi.org/10.1061/(ASCE)HE.1943-5584.0001756.

Matida, E. A., Nishino, K., Torii, K., 2000. Statistical simulation of particle deposition on the wall from turbulent dispersed pipe flow. Int. J. Heat Fluid Flow. 21 (4), 389 - 402. https://doi.org/10.1016/S0142-727X(00)00004-7.

714 Murphy, E., Ghisalberti, M., Nepf, H., 2007. Model and laboratory study of dispersion
715 in flows with submerged vegetation. Water Resour. Res. 43 (5), 687-696.
716 https://doi.org/10.1029/2006WR005229.
717 Nepf, H., Ghisalberti, M., 2008. Flow and transport in channels with submerged vege-
718 tation. Acta Geophys. 56 (3), 753-777. https://doi.org/10.2478/s11600-008-0017-
719 y.
720 Nepf, H., 1999. Drag, turbulence, and diffusion in flow through emergent vegetation.
721 Water Resour. Res. 35 (2), 1985-1986. https://doi.org/10.1029/1998WR900069.
722 Nepf, H., 2004. Vegetated flow dynamics. In The Ecogeomorphology of Tidal Marshes
723 (eds S. Fagherazzi, M. Marani and L. K. Blum), 137-163.
724 https://doi.org/10.1029/CE059p0137.
725 Nepf, H., 2012. Flow and transport in regions with aquatic vegetation. Annu. Rev. Fluid
726 Mech. 44 (1), 123-142. https://doi.org/10.1146/annurev-fluid-120710-101048.
727 Nepf, H., Sullivan, J. A., Zavistoski, R. A., 1997. A model for diffusion within emer-
728 gent vegetation. Limnol. Oceanogr. 42 (8), 1735-1745.
729 https://doi.org/10.4319/lo.1997.42.8.1735.
730 Pal, D., Ghoshal, K., 2016. Effect of particle concentration on sediment and turbulent
731 diffusion coefficients in open-channel turbulent flow. Environ. Earth Sci. 75 (18),
732 1245. https://doi.org/10.1007/s12665-016-6045-z.
733 Poggi, D., Katul, G. G., Albertson, J. D., 2004. A note on the contribution of dispersive
734 fluxes to momentum transfer within canopies. Bound.-Layer Meteor. 111(3), 615-
735 621. https://doi.org/10.1023/B:BOUN.0000016563.76874.47.

736 Raupach, M. R., Finnigan, J. J., & Brunei, Y., 1996. Coherent eddies and turbulence in
737 vegetation canopies: The mixing-layer analogy. Bound.-Layer Meteor. 78 (3-4),
738 351-382. https://doi.org/10.1007/BF00120941.
739 Ross, O. N., Sharples, J., 2004. Recipe for 1-d lagrangian particle tracking models in
740 space-varying diffusivity. Limnol. Oceanogr. Meth. 2 (9), 289-302.
741 https://doi.org/10.4319/lom.2004.2.289.
742 Rouse, H., 1937. Modern conceptions of the mechanics of fluid turbulence. Trans.
743 ASCE. 102, 463-505.
744 Sabbagh-Yazdi, S. R., Jamshidi, M., 2013. Depth-averaged hydrodynamic model for
745 gradual breaching of embankment dams attributable to overtopping considering
746 suspended sediment transport. J. Hydraul. Eng. 139(6), 580-592.
747 https://doi.org/10.1061/(ASCE)HY.1943-7900.0000706.
748 Salamon, P., Fernandez-Garcia, D., 2006. A review and numerical assessment of the
749 random walk particle tracking method. J. Contam. Hydrol. 87 (3), 277-305.
750 https://doi.org/10.1016/j.jconhyd.2006.05.005.
751 Samadi, A., Amiri-Tokaldany, E., Davoudi, M.H., and Darby, S.E., 2011. Identifying
752 the effects of parameter uncertainty on the reliability of modeling the stability of
753 overhanging multi-layered, river banks. Geomorphology. 134(3-4), 483-498.
754 https://doi.org/10.1016/j.geomorph.2011.08.004.
755 Stone, B. M., & Shen, H. T., 2002. Hydraulic resistance of flow in channels with cylin-
756 drical roughness. J. Hydraul. Eng.-ASCE. 128 (5), 500-506.
757 https://doi.org/10.1061/(ASCE)0733-9429(2002)128:5(500).

758 Shi, H. R., Liang, X. R., Huai, W. X., Wang, Y. F., 2019. Predicting the bulk average
759 velocity of open-channel flow with submerged rigid vegetation. J. Hydrol. 572,
760 213-225. https://doi.org/10.1016/j.jhydrol.2019.02.045.
761 Termini D., 2019. Turbulent mixing and dispersion mechanisms over flexible and dense
762 vegetation. Acta Geophys. 67, 961-970. https://doi.org/10.1007/s11600-019-
763 00272-8.
764 Thom, A. S., 1971. Momentum absorption by vegetation. Q. J. R. Meteorol. Soc. 97
765 (414), 414-428. https://doi.org/10.1002/qj.49709741404.
766 van Rijn, L. C., 1984. Sediment transport, part ii: Suspended load transport. J. Hydraul.
767 Eng. 110 (11), 1613-1641. https://doi.org/10.1061/(ASCE)0733-
768 9429(1984)110:11(1613).
769 Visser, A., 1997. Using random walk models to simulate the vertical distribution of
770 particles in a turbulent water column. Mar. Ecol. Prog. 158 (8), 275-281.
771 https://doi.org/10.3354/meps158275 .
772 Wang, G., Ni, J. R., 1990. Kinetic theory for particle concentration distribution in two-
773 phase flow. J. Eng. Mech. 116 (12), 2738-2748.
774 https://doi.org/10.1061/(ASCE)0733-9399(1990)116:12(2738).
775 Wang, X. Y., Xie, W. M., Zhang, D., He, Q., 2016. Wave and vegetation effects on
776 flow and suspended sediment characteristics: A flume study. Estuar. Coast. Shelf
777 Sci. 182, 1-11. https://doi.org/10.1016/j.ecss.2016.09.009.
778 Wilson, J. D., Yee, E., 2007. A critical examination of the random displacement model
779 of turbulent dispersion. Bound.-Layer Meteor. 125 (3), 399-416.

https://doi.org/10.1007/s10546-007-9201-x.

Zhong. D. Y., Zhang, L., Wu, B. S., Wang, Y., 2015. Velocity profile of turbulent sediment-laden flows in open-channels. Int. J. Sediment Res. 30 (4), S1001627915000530. https://doi.org/10.1016/j.ijsrc.2014.09.005.

Zhang, R., Xie, J. H., 1989. River sediment dynamics (in Chinese). China Water and Power Press. ISBN: 9787801244260.

Zhang, S. Y., Duan, J. G., Strelkoff, T. S., 2013. Grain-scale nonequilibrium sediment-transport model for unsteady flow. J. Hydraul. Eng. 139(1), 22-36. https://doi.org/10.1061/(ASCE)HY.1943-7900.0000645.